Physical Modeling Study on the Mixing in the New IronArc Process

Kristofer Bölke, Mikael Ersson, Peiyuan Ni, Maria Swartling, and Pär G. Jönsson*

IronArc is a newly developed technology for pig iron production with the aim to reduce the CO_2 emission and energy consumption, compared to a conventional blast furnace route. In order to understand the fluid flow and stirring in the IronArc reactor, water modeling experiments are performed. Specifically, a down scaled acrylic plastic model of the IronArc pilot plant reactor is used to investigate the mixing phenomena and gas penetration depth in the liquid bath. The mixing time is determined by measuring the conductivity in the bath, after a sodium chloride solution is added. Moreover, the penetration depth is determined by analyzing the pictures obtained during the experimental process by using both a video camera and a high speed camera. The results show that the bath movements are strong and that a circular movement of the surface is present. The mixing in the model for the flow rate of 282 NL min^{-1} is fast. Specifically, the average mixing times are 7.6 and 10.2 s for a 95% and a 99% homogenization degree, respectively. This is 15% and 18% (per degree of homogenization) faster compared to the case when using 3 gas inlets and the same flow rate.

1. Introduction

Small scale water model experiments are commonly used to investigate processes and phenomena's in steel production. This is due to that some phenomena are normally either difficult or expensive to be directly investigated in real production processes, due to the prevailing extreme conditions.

IronArc is a future new technology for pig iron production, which is developed by ScanArc in Sweden.[1] Currently, this process exists in a pilot scale, as seen in **Figure 1**a. In this process, hematite and magnetite are charged into the cylindrically-shaped reactor. This material is melted and a slag is created, when a hot carrier gas is injected through a plasma generator. The plasma generator (PG) heats the gas mixture of air and LPG (Liquefied Petroleum Gas) to a very high temperature, which is approximately 20 000 °C in the PG. Thereafter, it is injected into the slag with a temperature of 3500–4000 °C. The temperature drop of the injected gas is fast when it leaves the PG. The created CO-gas from the LPG is used as the reductant for the first reduction step to transform hematite and magnetite to wustite. Then, the FeO slag will be further reduced into Fe by using carbon as the reductant. The reactions that occur during this process are shown in Equation (1–3).

$$Fe_3O_4 + CO = 3FeO + 2CO_2 \quad (1)$$

$$Fe_2O_3 + CO = 2FeO + CO_2 \quad (2)$$

$$FeO + C = Fe + CO \quad (3)$$

This process has several advantages when producing pig iron. Specifically, the plasma generator is completely driven on electric energy, which gives the opportunity to use renewable resources as the input energy. In addition, a wide range of shapes of materials can be charged into the reactor. Therefore, the requirements on the physical properties of the material is of lesser importance, compared to the existing technologies for pig iron production where some of the materials need to be sintered together.[2] In addition, preliminary calculations show that this future new technology has the possibility to reduce the CO_2 emissions by approximately 50% and the usage of coke compared to existing technology for pig iron production.[1]

Since this is a completely new process, the fluid flow and transport phenomena during this process have not been reported earlier. Therefore, it is meaningful and valuable to carry out studies to investigate these phenomena inside the reactor under various process conditions. This information will also be valuable in the scaling up of the process to a future industrial application.

Processes that use gas injection are important for the steel industry and are widely used within the metallurgy field. In the past, several physical modeling studies have been carried out to investigate gas injection in various converters (**Table 1**). Zhou et al.[3] studied the mixing and fluid flow in a 1:6 scale 30 ton converter vessel by using both physical modeling and mathematical modeling. It was found that the mathematical model results agreed well with the experimental results. Specifically, the difference in the mean mixing time was only 2.8% between the experiments and predictions.

An optimized scheme for the bottom tuyeres with an asymmetric configuration was tested to optimize the stirring

K. Bölke, Dr. M. Ersson, Dr. P. Ni, Prof. P. G. Jönsson
KTH-Royal Institute of Technology
SE-100 44, Stockholm, Sweden
E-mail: bolke@kth.se

Dr. M. Swartling
ScanArc Plasma Technologies AB
SE-813 21, Hofors, Sweden

DOI: 10.1002/srin.201700555

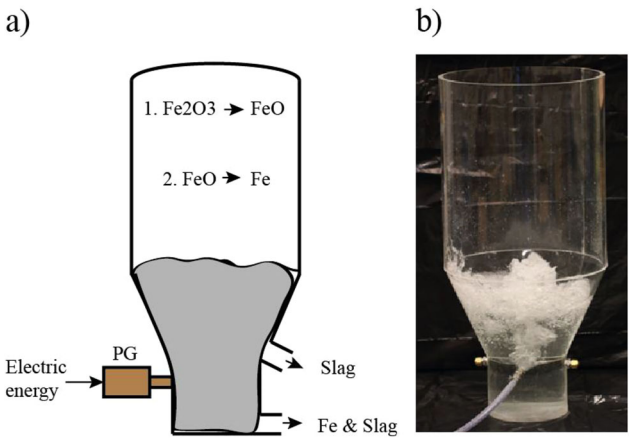

Figure 1. a) Schematic picture of the IRONARC pilot plant reactor in Hofors, Sweden. b) Water model and injected gas during the penetration depth measurements.

conditions when using combined top and bottom blown gas injection.[4] The asymmetric bottom blowing optimized scheme showed a decrease in mixing time for cases with different top lance heights and a constant bottom gas flow rate. The authors also used a combination of top, side, and bottom blowing to investigate if it was possible to reduce the splashing and mixing time by using blowing from a combination of three different gas inlet sources.[5] The results from the physical water modeling experiments showed a clear trend that the mixing time was reduced when a combined bottom and side blowing was used compared to when only bottom blowing was used. Furthermore, the results showed that the mixing time can be reduced further by increasing the flow rate using side blowing. A horizontal flow in the converter bath was obtained when the side blowing was introduced.

Visuri et al.[6] studied the mixing during the reduction step of a 1:9 scale physical model of the AOD process. The mixing time in the process was determined based on pH measurements, after that sulfuric acid had been added as a tracer. The mixing time under different gas blowing rates and positions of the tracer injection were studied. A mixing time equation including the tracer injection depth and gas flow rate was also proposed, which described the results reasonably well at a high gas flow rate. The results showed that the mixing time decreased with an increased volumetric air flow rate. Furthermore, that the mixing time increased when the tracer was injected at the location closer to the bath surface. Some other methods, besides conductivity measurements, have also been applied to determine the mixing time. Wupperman et al.[7] studied the mixing time in a 1/4 scale physical water model of a 120 ton AOD-converter. The tracer

Table 1. Examples of previous physical water model investigations of different converters in the steel industry.

Ref No.	Year	Author	Mixing time	Penetration depth	Gas blowing type[a)]	Conductivity measurements	Comparison of nr of inlets	Modified froude scaling	Model size	Air-water	Scale
3	2014	Zhou et al.	●		T	●		●	●	●	1:6
4	2014	Zhou et al.	●		T-B	●		●	●	●	1:6
5	2015	Zhou et al.	●	●	T-S-B	●		●	●	●	1:6
6	2016	Visuri et al.	●		S			●	●	●	1:9
7	2012	Wupperman et al.	●		S				●	●	1:4
8	2017	Samuelsson et al.	●		S		●	●	●	●	1:4.6
9	2010	Ternstedt et al.	●		S	●		●	●	●	
10	2004	Tilliander et al.			S			●	●	●	1:10
11	2005	Bjurström et al.		●	S			●	●	●	
12	1999	Wei et al.	●		S	●		●	●	●	1:3
13	2010	Wei et al.			T-S			●	●	●	1:4
14	2002	Wei et al.	●		S	●		●	●	●	1:3
15	2003	Fabritius et al.	●	●	S	●		●	●	●	
16	2010	Odenthal et al.	●	●	S			●	●	●	1:4
17	2001	Fabritius et al.	●	●	T-S	●			●	●	1:7
18	2013	Wuppermann et al.			S			●	●	●	1:4
19	2010	Wei et al.	●		T-S	●	●	●		●	
20	2004	Guthrie et al.		●	S		●	●	●	●	1:5

[a)] (Note: T = Top, B = Bottom, and S = Side)

used for the determination of mixing time was a food color and a photometer probe connected to a photometer was used to determine the concentration of the tracer in the water. Also, Samuelsson et al.[8] investigated the mixing time of a 1:4.6 scaled of a 120 t AOD vessel with the aim to increase the production capacity. Also, a comparison between 6 and 8 gas inlets were made. The results showed that the influence of the geometry of the converter on the mixing time was negligible. With an oblong converter vessel, the mixing time differed by less than 5% compared to a circular converter. Also, the average concentration deviation between the cases with 6 and 8 tuyeres was less than 1% after a stirring time of 165 s. Also, Ternstedt et al.[9] used physical modeling to investigate the mixing time in the AOD process. They found that the mixing time is dependent both on the gas flow rate and diameter of the converter. However, the influence of the bath depth was found to be negligible. An increase in vessel diameter resulted in an increased mixing time. Furthermore, an increased gas flow rate resulted in a decreased mixing time. Also, Tilliander et al.[10] developed a 3D mathematical model of the AOD converter, which could predict the gas plume of gas injection. In their work, physical modeling was performed to validate the mathematical model predictions. In addition, Bjurström et al.[11] investigated the fluid flow pattern and the penetration depth in a small scale physical model of a 100 ton AOD vessel. The penetration depth was investigated by using video recordings. It was found that both the penetration depth at the tuyere and the bath surface level were more dependent on the gas flow rate than on the bath depth. Besides the above discussed studies, several other examples exist where physical water modeling has been used for the investigation of fluid flow phenomena in metallurgical vessels and converters.[12–20]

In this work, small scale water modeling was used to investigate the behavior of the bath in the newly developed novel IronArc reactor. The mixing time and penetration depth were investigated for several different cases, which include different flow rates, number of inlets etc. The aim was to obtain a good understanding about the fluid flow and transport phenomena inside the new reactor, which is important for the process optimization as well as for future industrial applications.

2. Experimental Section

Water experiments were performed in a small 1:3 scale model. Both the penetration depth and the mixing time were determined. In addition, the overall movement of the bath was investigated. The dimensions of the small scale model can be seen in **Figure 2**.

2.1. Mixing Time

The model of the pilot plant was made of acrylic plastic. Thus, all the lengths in the model are 1/3 of the corresponding pilot plant reactor lengths in order to maintain a geometric similarity between the model and the pilot plant reactor. The dynamic similarity between the model setup and the pilot plant setup was realized by using the modified Froude number. It is defined as the ratio of inertial forces to the buoyancy forces (equation 4):

$$N_{\mathrm{Fr}'} = \frac{\rho_g u_0^2}{g\rho_l d_0} \tag{4}$$

where $N_{Fr'}$ is the modified Froude number, ρ_g (kg) and ρ_l (kg) are the density for the gas and the liquid, respectively. The parameter u_0 (m s^{-1}) is the velocity of the gas at the inlet, g (ms^{-2}) is the gravitational acceleration constant, and d_0 (m) is the characteristic length of the system. In this case, the characteristic length represents the diameter of the reactor. The flow rate was scaled based on Equation (5). This is frequently used for scaling of flow rates when the modified Froude number is used as the similarity criteria.[8–10]

$$\mathrm{Q}_m = \mathrm{Q}_R \lambda^{2.5} \tag{5}$$

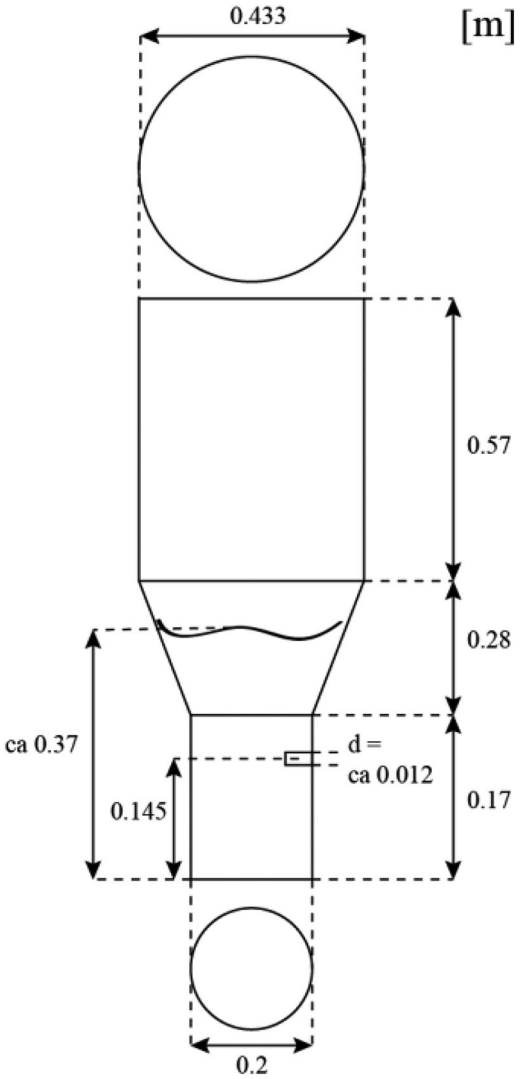

Figure 2. Dimensions of the acrylic plastic model used in the water model experiments for determinations of the penetration depths and mixing times.

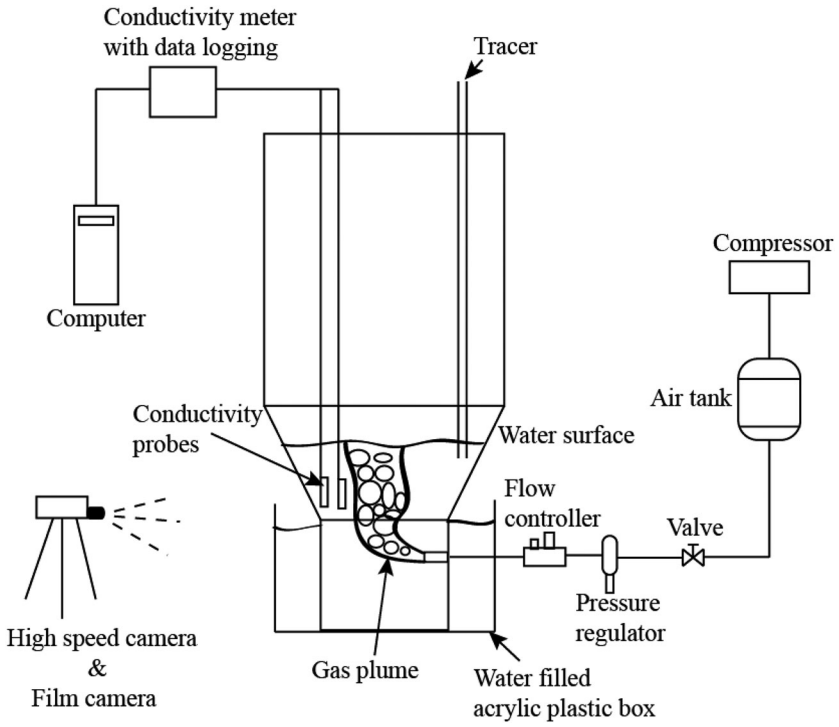

Figure 3. A schematic picture of the experimental setup used in the mixing time and penetration depth experiments.

where Q_m (m^3s^{-1}) is the flowrate for the downscaled model, Q_R (m^3s^{-1}) is the flowrate in the real process, and λ is the scale factor with the value of 1/3 in this case. The diameter of the inlet was determined from the following equation, when both the velocity and flow rate were given:

$$Q = \frac{u\pi d^2}{4} \tag{6}$$

The mixing time is defined as the time it takes to homogenize a liquid content in a tank, to a chosen degree of homogenization after a step change in the composition has been reached. Specifically, the mixing time, was defined as the time for the bath to reach a homogenization degree of 95% of the final tracer content after a tracer element had been added to the bath. Specifically, for the uniformity value, H, to reach values between 0.95 and 1.05. In addition, the time to reach a 99% homogenization degree in the bath was determined. The definition of H can be seen in Equation (7):

$$H = \frac{C(t)}{C_f} \tag{7}$$

where H is the degree of homogenization, $C(t)$ is the concentration at time t, and C_f is the final concentration value in the water after a complete homogenization. The tracer concentration is measured and determined at various locations in the water bath. In some cases, the mean value of the measurements at the different positions is applied to obtain the mixing time.[3–5]

In the experiments, water was used as the liquid and compressed air as the gas. The experimental set up can be seen in **Figure 3**. The compressed air was blown in to the water through a nozzle that was connected to the acrylic plastic wall. A flowmeter was connected to the tube, which measured and controlled the air flow rate. At the beginning of the experiment, a tracer solution consisting of a 20 wt% NaCl solution was added to the bath. Thereafter, the conductivity in the water was measured by using two conductivity probes. These were placed at different positions in the bath, as shown in **Figure 4**a. The probes used for conductivity measurement were equipped with temperature compensation, which means that the measured conductivity corresponds to a value at the reference temperature of 25 °C. The conductivity data was logged every second during the entire time of the measurements. The time required for the probes to measure a concentration reaching a 95% homogenization degree of the final concentration in the liquid bath was determined as the mixing time. The saline solution tracer was added to the water when the flow field was fully developed, since the blowing were done for a time that was several times longer than the mixing time for this process. The experimental parameters and conditions are given in **Table 2**.

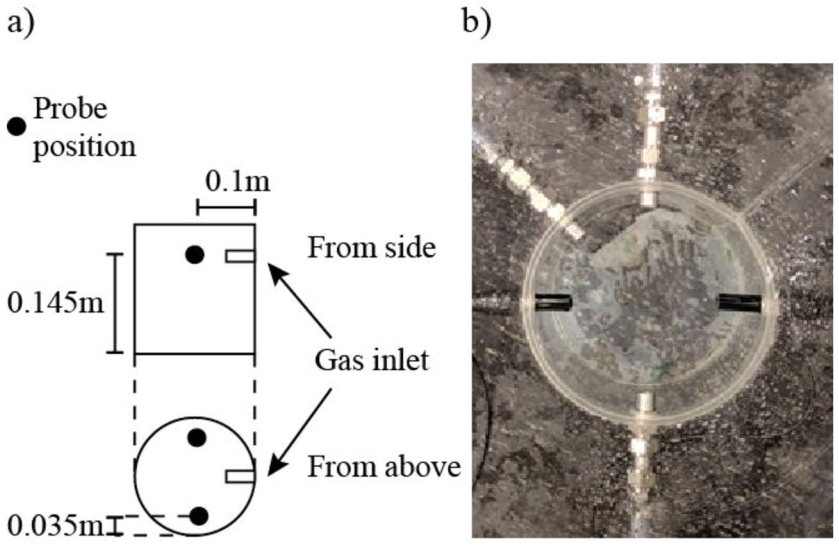

Figure 4. a) Position of conductivity probes in the water in the bottom part of the acrylic plastic model. b) The setup with three gas inlets seen from above.

Table 2. Parameters used in the physical water model experiments and in the real process.

Parameters	Physical water model	Real process
Scale	1:3	1
Flow rate ($Nm^3\ h^{-1}$)	17	265
Bath depth liquid (m)	0.37	1.1
Nozzle height location (m)	0.145	0.435
Density liquid ($kg\,m^{-3}$)	998.2	3562
Density gas ($kg\,m^{-3}$)	1.226	0.1887
Diameter of lower cylinder (m)	0.2	0.6
Diameter of upper cylinder (m)	0.433	1.3
Diameter tuyere (m)	0.0117	0.035

2.2. Penetration Depth

The gas plume in the bath was studied for different flow rates by using a high-speed camera (MotionBlitz Cube 4), with the capability of capturing 1000 frames per second, and a film camera (Panasonic HDC-TM900). The Penetration depth, which is the depth of the injected gas at the tuyere level, was measured by investigating both the video from the film camera as well as the pictures taken with the high speed camera. The setup, which can be seen in Figure 3, were similar as the one used for the mixing time experiments except for that no probes were present in the water. The penetration depth were determined for the following gas flow rates: 100, 200, 300, 400, 500, and 600 NL min^{-1}. The diameter of the tuyere inlet was 0.012 m. The bath height was also kept constant at a value of approximately 0.37 m. The model and the gas plume in the water are illustrated in Figure 1b. The penetration depths at the different flow rates were compared to the penetration depths by using an empiric equation suggested by Oryall and Brimacombe[21]:

$$l_p = 10.7 N_{Fr'}^{0.46} d_0 \left(\frac{\rho_g}{\rho_l}\right)^{0.35} \quad (8)$$

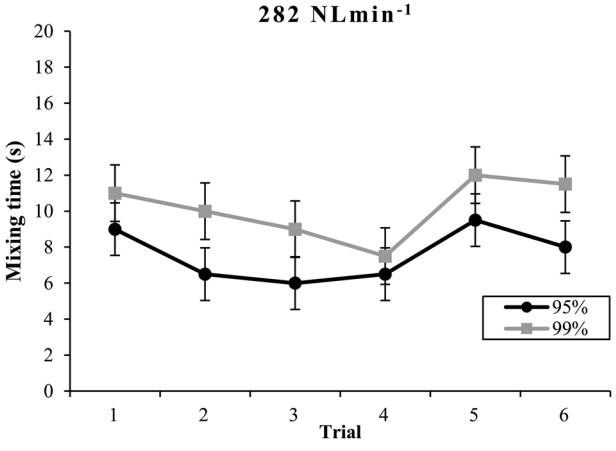

Figure 5. Measured mixing times for a flow rate of 282 NL min^{-1} for both a 95% and a 99% degree of tracer homogenization.

where l_p is the penetration depth, $N_{Fr'}$, is the modified froude number, d_0 (m) is the diameter of the inlet, ρ_g and ρ_l (kgm^{-3}) are the density of the gas and liquid, respectively. This relationship is frequently used in the literature.[16,22]

3. Results and Discussion

3.1. Mixing Time

The mixing time was determined in a small scale acrylic plastic model of the IronArc process. The time for the bath to be homogenized was determined by measuring the conductivity over time, after a sodium chloride solution was added to the bath. The mixing time was measured for a flow rate of 282 NL min^{-1}. This corresponds to a flow rate of 265 $Nm^3\ h^{-1}$, which is the average flow rate used in the pilot plant reactor. Six trials were performed for this experiments (**Figure 5**). Measurements were made for different flow rates to investigate the influence of the flow rate on the mixing time.

The results for the mixing time for a 282 NL min^{-1} flow rate can be seen in Figure 5. This figure shows the six repeated trials focusing on mixing time measurements, when using one inlet and the setups shown in Figure 3 and 4a. Tracer additions were made at the same position in the bath for all trials. The time for both 95% as well as 99% homogenization degrees, as defined in Equation (4), were determined. As can be expected, the mixing time is longer (34% longer when comparing the average mixing time for all cases for both homogenization degrees, respectively) for a 99% homogenization degree compared to a 95% homogenization degree. The same trends were found for all trials. However, there are small deviations in the results among the trials. For a 95% homogenization degree, the mixing time varies between 9.5 and 6 s with an average mixing time of 7.6 s. The results for a 99% degree homogenization degree also show a small deviation in mixing time. Specifically, the maximum and minimum values are, 12 and 7.5 s, respectively. Furthermore, the average value is 10.2 s.

In **Figure 6**a, the mixing times for three different flow rates are shown. It can be seen in the figure that longer times were required to reach a 99% homogenization degree was required compared to a 95% homogenization degree, for all the tested flow rates (122, 282, and 400 NL min^{-1}). A flow rate of 600 NL min^{-1} was also tested, but unfortunately the probe position was not optimal for this high flow rate due to the interruption of the air bubbles on the electrodes at the probe tips. These results also show that an increase in flow rate decreases the mixing time, which is expected due to an increase in velocity of the injected gas as well as due to an increase of the buoyancy effect. This has been shown in earlier studies.[11]

A typical tracer concentration curve can be seen in **Figure 7**a. It shows the tracer concentrations for the two probes in the water after an addition of the saline solution. In Figure 7b, the same curve is shown but for a narrower interval. Thereby, it is possible to observe that the tracer concentration reached homogenization degrees of 95% and 99%. The flow in the water bath was strong and turbulent. Also, periodic circular movements of the bath could be observed at the reactor wall. The tracer solution was added approximately at the same spot during all trials.

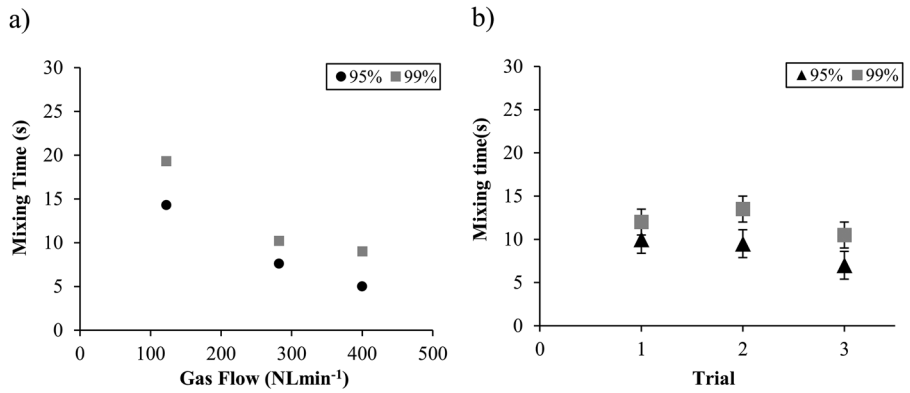

Figure 6. a) Mixing times for different flow rates when using one gas inlet. b) Mixing times for experiments using three gas inlets. Data are presented for both 95% and 99% homogenization degrees.

Furthermore, the gas blowing lasted during the same amount of time before the tracer was added. However, the position varied with an approximate area of a circle with diameter of 3 cm. This was due to that the tracer was poured into the bath. Also, depending on when the tracer was added, the bath surface will be different. Thus, the height could be different for the different trials. This is due to the circulating movement of the bath surface, the irregularities of the surface waves, and in turn the differences in bath heights at the position where the tracer was added. Also, the bath is in an intensive dynamic state during the gas injection. This is due to the circulating movement of the bath surface, the irregularity of the surface waves, and in turn the change of bath height. Therefore, it is difficult to guarantee a completely similar situation during the tracer addition for each trial. This may result in a difference of the spreading of the sodium chloride solution in the bath and hence result in differences between the measurements. However, the mixing times for both the 95% and 99% homogenization degrees are very small, with average values of 7.6s and 10.2 s respectively. This means that the mixing in this process is extremely powerful. This, in turn, is a very positive result since it shows that one of the advantages of this process is an intensive mixing.

The effect of the tuyere number on the mixing time was determined for a gas flow rate of 282 NL min^{-1}, which corresponds to the average gas flow rate of the flow rate used in the pilot plant reactor. Three tuyeres were used and each had a diameter of 0.0117 m. Three trials were performed in the same way as was done for the trials when using multiple inlets: The result for the mixing time can be seen in Figure 6b. The probe positions were the same as in Figure 4a and the tracer was added at approximately the same place as in the trials with one inlet. The inlet position, as well as the position of the conductivity probes can be seen in Figure 4b. The position for tracer addition varied in an area with a radius of approximately 3 cm. The purpose of these trials was to investigate whether the number of nozzles have an impact on the mixing time, when using the same gas flow rate. Even though the mixing time have been investigated earlier by using water modeling, it is not common that the effect of the tuyere number on the mixing has been investigated. Samuelsson et al.[8] investigated the influence of the nozzle number on the mixing time for an oblong converter, by using a small scale AOD model. Their results showed that the amount of tuyeres has an insignificant effect on the mixing time, when comparing the use of 6 and 8 tuyeres. The tuyeres were

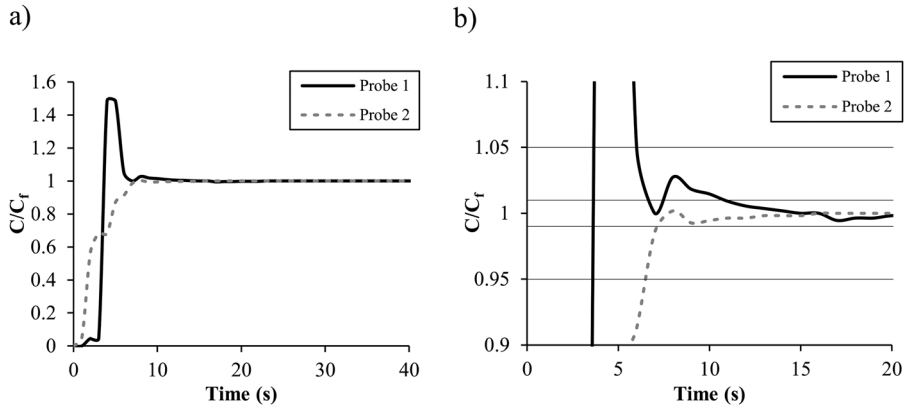

Figure 7. Data of normalized conductivity curves for two probes. This measurements was from the third trial when using one gas inlet. a) Shows the normalized conductivity value from 0 to 1.6. b) Shows the normalized conductivity value from 0.9 to 1.1. Horizontal lines that shows the areas for 95% and 99% degrees of homogenization.

positioned at the same side wall in the oblong converter. However, in this work the mixing time significally increases in the case with 3 tuyeres compared to the case with 1 tuyere. The increase in the average values of the mixing times for a 95% homogenization degree and for a 99% homogenization degree were 15.8% and 17.6%, respectively. A likely explanation to these results is that the bath surface was much more stable and calm when 3 tuyeres were used, compared to when one tuyere was used. Specifically, when using one inlet, the movement of the surface was violent and more powerful. This, in turn, resulted in a circular movement of the bath as described earlier. This movement will influence the stirring of the bath and make the tracer distribution in the bath faster. This theory is supported by the result shown by Zhou et al.,[5] which showed that the mixing time decreases when submerged gas injection is inserted into a top and bottom blown converter. Also, an increase in the flow rate from the side blowing tuyeres was found to further decrease the mixing time. This decrease may be due to the fact that the side blowing increases the radial velocity and the horizontal flow in the bath, which in turn increases the bath mixing and reduces the mixing time. Even though the mixing time increased with 3 tuyeres, the tracer in the bath was still homogenized in a short time. More specifically, a 95% homogenization degree was reached 8.8 s after a tracer addition was made and the value for a 99% homogenization degree was 12 s. For the 3 inlet case, two of the tuyeres were placed at positions direct opposite to each other and on different sides of the model. Thus, they works as a counterpart to each other so that the circular movement of the surface is greatly reduced. It becomes more of an extreme case when comparing 3 and 1 gas inlets, with inlets placed on opposite sides to each other, compared to 6 and 8 inlets positioned at the same side, as investigated by Samuelsson et al.[8] With the same flow rate for the three inlet case, the flow rate per inlet was one third compared to when only one inlet was used. Hence, the velocity per inlet was reduced to 14.7 m s^{-1} compared to 44 m s^{-1} for the one-inlet case. This, in turn, resulted in a shorter penetration depth of the air into the water for the three-inlet case compared to the one-inlet case.

It is also important to discuss the physical properties of water versus slag. The slag and water differs in kinematic viscosity.

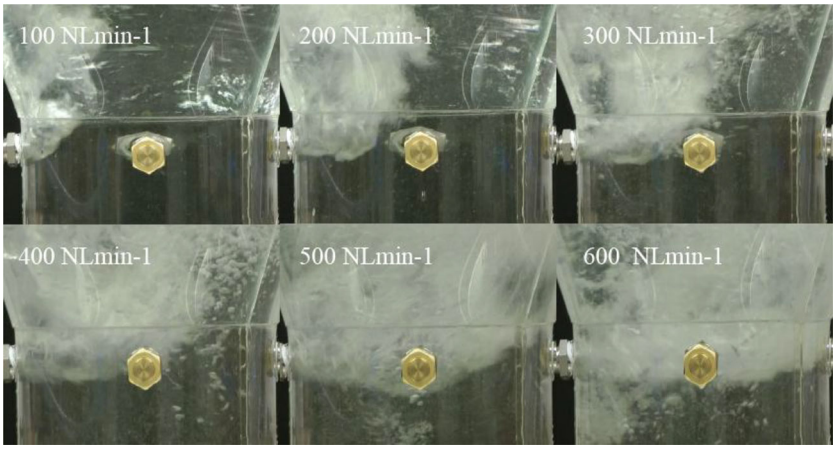

Figure 8. The measured air plume in the water for all tested flowrates.

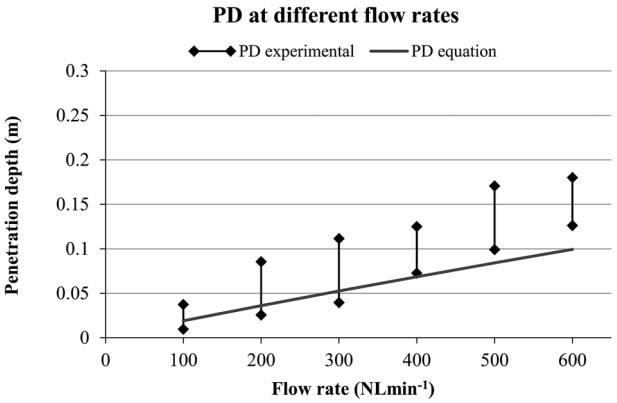

Figure 9. Penetration depths determined both experimentally and using the empiric equation at different flow rates. The experimental lines shows the max and min values at each flow rate.

Specifically, the kinematic viscosity of slag is higher than that of water by approximately one order of magnitude. This is based on calculations using an estimated dynamic viscosity of the slag of 0.0035 m^2 s^{-1} and an approximate density of 3500 kg m^{-3}. The kinematic viscosity of the water that is 10^{-6} m^2 s^{-1}. According to Iguchi et al.,[23] the kinematic viscosity affects the mixing efficiency and in turn the mixing time, in a bottom blown converter. The authors states that a higher value of the kinematic viscosity will result in an increased mixing time. However, the maximum gas flow rate for the bottom blown reactor when examining the mixing time for higher viscosity oils were in the range of 10^{-4} m^3 s^{-1}. This is 48 times lower than the flowrate of 0.0048 m^3 s^{-1} used in this investigation. In addition, Iguchi et al. tested two different sizes of containers for the bottom blowing investigations with oils. The results for both vessels shows a tendency that an increased flow rate leads to a decreased difference in mixing time between the different fluids with different kinematic viscosities. This is more clearly seen for the larger vessel diameter of 0.2 m. Since data are lacking for higher flow rates it is not possible to say how an increased kinematic viscosity will affect the mixing time at higher flow rates. However, it is clear that a higher flow rate will result in a more turbulent flow, which will lead to an increased effective viscosity. Also, the turbulent viscosity is several orders of magnitude greater than the kinematic viscosity and it has been stated that in highly turbulent flows the liquid viscosity does not influence the main overall movement of the fluid medium.[24] Hence, the mixing efficiency will be much more dependent on the turbulent viscosity than on the kinematic viscosity for a bath with high gas flow rate. Due to the turbulent characteristics of this flow the kinematic viscosity should not influence the mixing time to a large extent. Instead, it will be more dependent on the turbulent viscosity of the flow. It should also be noted that the current study the pilot plant slag

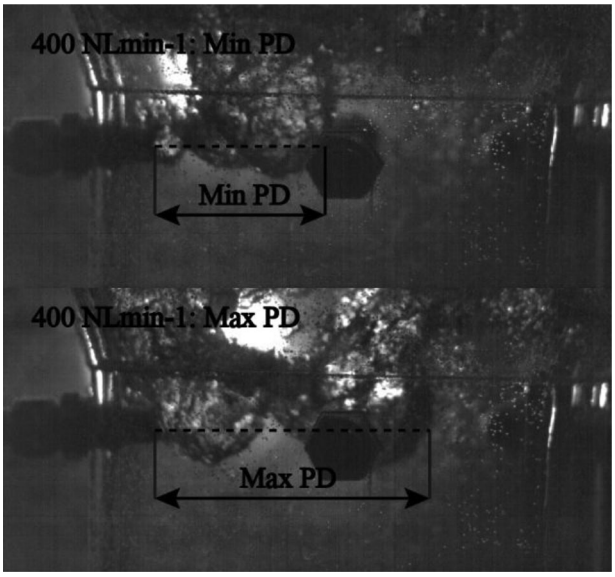

Figure 10. The penetration of the air in the water for a flowrate of 400 NL min^{-1}. Data are presented for the minimum penetration (upper figure) and the maximum penetration (lower figure).

process and the water model have similar values of the modified Froude numbers. Thus, the ratio of inertial forces over buoyancy forces are equal.

3.2. Penetration Depth

Water model experiments were also performed to determine the penetration depth by taking photographs and filming with a high speed camera and a video camera. The pictures and films were analyzed and the penetration of the air into water were determined at different flow rates. This can be seen in **Figure 8**, where the penetration of the gas and the gas plume in the water is shown for the different flow rates. In **Figure 9**, the penetration depths at different flow rates from the experiment are compared to predictions using an empirical equation suggested by Oryall and Brimacombe.[21] The velocity of the gas at the inlet was determined by considering the flowrate and the area of the inlet. Note, that the penetration depth does not have a constant value. Instead, it shows sort of a pulsating behavior, where the different pulses penetrates different distances into the water. These results are similar as the results reported by Oryall.[25] This is illustrated in Figure 9, where the bars in the plot show the minimum and maximum penetration depths at each tested flow rate. It should be mentioned that these pulses appears less than a second apart from each other. Therefore, they are quite difficult to see when observing the flow without using a high speed camera, but are nonetheless visible.

Figure 10 shows the flowrates for the approximate max and min penetration depths captured at different pulses for a flowrate of 400 NL min^{-1}. The length of penetration differs clearly, from a minimum value of 7.3 cm to a maximum value of 12.5 cm. The pulses showed some kind of repetitive pattern, where a pulse with a long penetration was followed by a pulse with a short penetration. Due to these differences in penetration depths that appeared for the same flowrate, it is difficult to determine the actual penetration depth. When comparing the experimental results to the predictions using the empirical equation, the lower penetration depth seems to fit the empirical Equation (8) better for gas flow rate values of up to around 400 NL min^{-1}. However, for flow rates from 500 up to 600 NL min^{-1} the penetration depths from the experiments differs, more clearly, from the penetration depths from the empirical equation, even for the shortest pulses.

Both the experiments and the predictions show the same tendency with respect to that an increased gas flow rate results in an increased penetration depth. This is expected, due to that the gas will have a higher velocity at the inlet for an increased flow rate. Also, the pulses were more visible and more accurately determined lengthwise for the shorter penetration depth as well as for the lower flow rates, compared to the pulses found at the higher flowrates. In the latter case, the air from the longer penetration of a pulse were still in front. Furthermore, they rose more slowly in the vertical direction than for the next following shorter pulse, which penetrated the water horizontally. Since the same diameter of the inlet is used for all flow rates tested, the modified Froude number (Eq. 4) will increase as the flow rate increases. Overall, the empirical equation (Eq. 8) by Oryall and Brimacombe is, according to these results, more fitted to use for lower Froude numbers than for higher Froude numbers.

Due to the large flow rate for the relatively small amount of water used, the surface of the water will move and the height of the water at the different walls will vary. This will result in different pressures at the inlet, as the water height above it increases or decreases. It is also possible that the flow meter will provide a larger amount of air as the pressure above the inlet increases, which will cause the gas to penetrate a longer distance into the liquid.

It is important to consider the reflections of the lights through the 1.2 cm thick acrylic plastic wall, which is curved due to the cylindrical shape of the water model. To reduce the reflections from the curved acrylic plastic wall, an outer box made of acrylic plastic was used. This was also filled with water to reduce the reflections from the curved surface. This is due to that the flat surface is perpendicular to the filming direction. This, in turn, gives a more representative vision of the plume compared to when observing the plume through the curved glass wall. The powerful stirring for the higher flowrates creates many bubbles in the plume area and around it. This impairs the vision of the plume, when investigating the pictures from the high speed camera. This is due to that the light does not penetrate the bubbles to a high extent.

The flow rate off 300 NL min^{-1} is just a little bit larger than that of 282 NL min^{-1}, which is scaled from the average flow rate of the pilot plant reactor. This means that according to this result, the penetration depth corresponding to the pilot plant flow rate would be slightly lower than the penetration depth span of 0.04–0.011 m for the 300 NL min^{-1} flow rate. Therefore, the gas plume will not rise at the opposite wall. Hence, the refractory wear should be less on that wall compared to a case with a longer penetration depth. Also, the shorter pulses of the depth will be slightly smaller than 0.04 m, which also means that the plume will not rise directly at the tuyere wall. This is also positive, since it results in less refractory wear at that wall.

The energy usage in the gas is also affected in a positive way, if the gas plume rises at a distance away from the wall, since a larger volume of the plume will be used to stir the bath. The injected gas in the pilot plant reactor is a reductant which is used during the first reduction step in the reactor. Hence, there will be gas formations during the reduction when the created CO from the LPG reacts with the slag. However, the gas formation during the reduction was not taken into account, when simulating the penetration depth in the cold water experiments. The reason is because the gas will only react during the first reduction step in the pilot plant reactor, when hematite and magnetite are reduced to wustite. From a practical experience, it is believed that this reduction step happens fast. The injected gas consists of a mixture of gas and liquefied petroleum gas, where the large majority of the gas is air. The air over LPG ratio is around 20–25, which means that the amount of gas that reacts represents a small part of the total volume of the injected gas. Therefore, it should not influence the penetration depth.

4. Conclusions

Water model experiments were performed in a small scale acrylic plastic model, scaled as a 1:3 ratio of a newly developed IronArc pilot plant reactor. Both the mixing times and penetration depths were investigated under different conditions, due to their importance to the process. The mixing time was determined by measuring the conductivity in the water, after a sodium chloride solution was added to the bath. Furthermore, the penetration depth was investigated by using a video camera and a high speed camera. The conclusions that can be drawn from the results regarding the mixing time and the penetration depth are the following:

The mixing in the small scale model is fast, with the average mixing times of 7.6 and 10.2 s for a 95% and a 99% homogenization degree, when one inlet and a flow rate of 282 NL min^{-1} was used. A strong flow was created in the bath and it had a periodic movement that caused the water to circulate around the walls in the model. This movement of the surface was not observed to the same extent for the 3 inlet case compared to a case with one inlet. Also, when several tuyeres were used, the flow was calmer. This resulted in that the strong surface movements were greatly reduced. This may explain the longer mixing times for a flow rate of 282 NL min^{-1} for the three-inlet case compared to the one-inlet case. The average mixing times with three gas inlets were 8.8 and 12 s for 95% and 99% homogenization degrees, respectively. So, there are a 15.8% and a 17.6% increase in the mixing time for the 95% and 99% degrees of homogenizations, when using multiple gas inlets compared to a gas injection when using only one inlet. However, the mixing in the small scale IronArc pilot plant is fast regardless of the two different setups tested. Further results showed that an increased flow rate resulted in a reduced mixing time.

The penetration depth was measured and determined at several different flow rates. The results showed that the penetration depth increases with an increased flow rate. When the results were compared to an empiric equation from the literature, the results agreed better for low gas flow rates compared to high gas flow rates. In the latter case, the penetration depths were longer than those predicted by using the empiric equation. Also, the penetration at the tuyere center line showed a pulsating behavior where a pulse that penetrated a longer distance was followed by a pulse with shorter penetration. The length difference between the pulses also increased with an increased flow rate.

For a flow rate of 100 NL min^{-1}, the maximum difference between the measured penetration depth and the empiric equation was a 95% longer penetration depth for the measured penetration depth value. That difference increased for a flow rate of 500 NL min^{-1}, where the measured value was estimated to be 103% longer for the longest pulse at this flow rate, compared to the penetration depth obtained from the empiric equation. Also, for a flow rate of 100 NL min^{-1} the predicted penetration depth was longer than for the shortest pulse of the measured penetration depth value, with a length of approximately two times the measured value. However, for the flow rate of 500 NL min^{-1} the shortest penetration was longer than the predicted penetration depth for the same flow rate by approximately 18%.

The maximum penetration depth of the air for the flow rate off 300 NL min^{-1} was determined to have a value of 0.11 m. This means that the maximum penetration depth for the flow rate of 282 NL min^{-1} (a scaled flowrate corresponding to average flow rate of the pilot plant) will be slightly smaller. This, in turn, indicates that the gas plume will not reach to the opposite wall of the cylindrical bath.

Acknowledgements

The author wish to thank the Swedish Energy Agency for the financial support. Also, the personnel at ScanArc for their valuable help and hospitality during the visits to the facility of the pilot plant in Hofors, Sweden.

Conflict of Interest

The authors declare no conflict of interest.

Keywords

Blast Furnace, CO_2 Reduction, IronArc Process, Ironmaking, Mixing, Pig Iron Production

Received: December 20, 2017
Revised: March 1, 2018
Published online: April 6, 2018

[1] S. Santen, M. Imris (ScanArc Plasma Technologies AB) Swe. *SE 536 291 C2*, **2013**.
[2] J. G. Peacey, W. G. Davenport, *The Iron Blast Furnace Theory and Practice*, Pergamon Press, Canada **1979**.
[3] X. Zhou, M. Ersson, L. Zhong, J. Yu, P. G. Jönsson, *Steel Res. Int.* **2014**, *85*, 273.
[4] X. Zhou, M. Ersson, L. Zhong, J. Yu, P. G. Jönsson, *ISIJ Int.* **2014**, *54*, 2255.
[5] X. Zhou, M. Ersson, L. Zhong, J. Yu, P. G. Jönsson, *Steel Res. Int.* **2015**, *85*, 1.

[6] V. Visuri, E. Isohookana, A. Kärnä, T. Haas, R. H. Eriç, T. Fabritius, *5th Int. Conf. on Process Development in Iron and Steelmaking*, Luleå, Sweden, June **2016**.
[7] C. Wupperman, N. Giesselmann, A. Rückert, H. Pfeifer, H. Odenthal, *ISIJ Int.* **2012**, *52*, 1817.
[8] P. Samuelsson, P. Ternstedt, A. Tilliander, A. Apell, P. G. Jönsson, *Ironmaking Steelmaking* **2017**, *44*, 1.
[9] P. Ternstedt, A. Tilliander, P. G. Jönsson, M. Iguchi, *ISIJ Int.* **2010**, *50*, 663.
[10] A. Tilliander, T. L. I. Jonsson, P. G. Jönsson, *ISIJ Int.* **2004**, *44*, 326.
[11] M. Bjurström, A. Tilliander, M. Iguchi, P. G. Jönsson, *ISIJ Int.* **2006**, *46*, 523.
[12] J. H. Wei, J. C. Ma, Y. Y. Fan, N. W. Yu, S. L. Yang, S. H. Xiang, D. P. Zhu, *Ironmaking Steelmaking* **1999**, *26*, 363.
[13] J. H. Wei, H. L. Zhu, Q. Y. Jiang, G. M. Shi, H. B. Chi, H. J. Wang, *ISIJ Int.* **1999**, *39*, 779.
[14] J. H. Wei, *J. Shanghai Univ.* **2002**, *6*, 1.
[15] T. M. J. Fabritius, P. T. Mure, J. J. Harkki, *ISIJ Int.* **2003**, *43*, 1177.
[16] H. J. Odenthal, U. Thiedemann, U. Falkenreck, J. Schlueter, *Metall. Trans. B* **2010**, *41*, 396.
[17] T. M. J. Fabritius, P. A. Kupari, J. J. Harkki, *Scand. J. Metall.* **2001**, *30*, 57.
[18] C. Wupperman, A. Rückert, H. Pfeifer, H. Odenthal, *ISIJ Int.* **2013**, *53*, 441.
[19] J. H. Wei, H. L. Zhu, H. B. Chi, H. J. Wang, *ISIJ Int.* **2010**, *50*, 26.
[20] R. I. L. Guthrie, M. Isac, Z. H. Lin, *Ironmaking Steelmaking* **2005**, *32*, 133.
[21] E. O. Hoefele, J. K. Brimacombe, *Metall. Trans. B* **1979**, *10*, 631.
[22] M. Y. Zhu, I. Sawada, M. Iguchi, *ISIJ Int.* **1998**, *38*, 411.
[23] M. Iguschi, K. Nakamura, R. Tsujino, *Metall. Mater. Trans. B* **1998**, *29*, 569.
[24] K. Minsker, A. Berlin, V. Zakharov, G. Zaikov. *Fast Liquid-Phase Processes in Turbulent Flows*, CRC Press, Boston USA **2004**, p. 17.
[25] G. N. Oryall, J. K. Brimacombe, *Metall. Trans. B* **1976**, *7*, 391.